Original contribution

# Intramuscular adipose tissue determined by T1-weighted MRI at 3T primarily reflects extramyocellular lipids

Hiroshi AKIMA[1,2], Maya HIOKI[3], Akito YOSHIKO[3], Teruhiko KOIKE[1,3], Hisataka SAKAKIBARA[3], Hideyuki TAKAHASHI[4], Yoshiharu OSHIDA[1,3]

[1]Research Center of Health, Physical Fitness & Sports, [2]Graduate School of Education & Human Development, Nagoya University
1 Furo, Chikusa, Nagoya, Aichi 4648601, Japan

[3]Graduate School of Medicine, Nagoya University
65 Tsurumai, Showa, Nagoya, Aichi 4668550, Japan
1-1-20 Daiko-Minami, Higashi, Nagoya, Aichi 4618673, Japan

[4]Japan Institute of Sports Sciences
3-15-1 Nishigaoka, Kita, Tokyo 1150056, Japan

Running head: Intramuscular adipose tissue

Corresponding and reprint request: Hiroshi AKIMA, PhD
Research Center of Health, Physical Fitness & Sports, Nagoya University
Furo, Chikusa, Nagoya, Aichi 4648601, Japan
Phone +81(52)789-3954, Fax +81(52)789-3957
e-mail akima@nagoya-u.jp

**Abstract**

**Purpose:** The purpose of this study was to assess relationships between intramuscular adipose tissue (IntraMAT) content determined by MRI and intramyocellular lipids (IMCL) and extramyocellular lipids (EMCL) determined by $^{1}$H-magnetic resonance spectroscopy ($^{1}$H-MRS) or echo intensity determined by B-mode ultrasonography of human skeletal muscles.

**Methods:** Thirty young and elderly men and women were included. T1-weighted MRI were taken from the right mid-thigh to measure IntraMAT content of the vastus lateralis (VL) and biceps femoris (BF) using a histogram shape-based thresholding technique. IMCL and EMCL were measured from the VL and BF at the right mid-thigh using $^{1}$H-MRS. Ultrasonographic images were taken from the VL and BF of the right mid-thigh to measure echo intensity based on grey-scale level for quantitative analysis.

**Results:** There was a significant correlation between IntraMAT content by MRI and EMCL of the VL and BF (VL, $r = 0.506$, $P < 0.01$; BF, $r = 0.591$, $P < 0.001$) and between echo intensity and EMCL of the VL and BF (VL, $r = 0.485$, $P < 0.05$; BF, $r = 0.648$, $P < 0.01$). IntraMAT content was also significantly correlated with echo intensity of the VL and BF (VL, $r = 0.404$, $P < 0.05$; BF, $r = 0.493$, $P < 0.01$).

**Conclusion:** Our study suggests that IntraMAT content determined by T1-weighted MRI at 3T primarily reflects extramyocellular lipids, not intramyocellular lipids, in human skeletal muscles. (230 words)

Key words: intramuscular adipose tissue, spin-echo sequence, extramyocellular lipids, intramyocellular lipids, ultrasonography, image analysis

## 1. Introduction

Adipose tissue infiltrates within the muscle and accumulates as a result of aging [1-4], inactivity [5, 6], obesity [7-10], or myopathy [11-13]. Although intermuscular adipose tissue is typically the broadest definition of adipose tissue infiltration in the muscle, referring to storage of lipids in adipocytes underneath the deep fascia of muscle [14], this study focuses on adipose tissue within a muscle, that is intramuscular adipose tissue (IntraMAT). The physiological and biochemical roles of IntraMAT are not fully understood; however, it is described as a unique adipose tissue depot that has a similar function to visceral adipose tissue in terms of representing risks for metabolic impairment such as type 2 diabetes [7, 8, 14-16] and as an index for progression of muscular dystrophy [11-13].

IntraMAT has been evaluated using medical imaging techniques such as magnetic resonance imaging (MRI) and B-mode ultrasonography (US), and using a spectrum technique such as $^{1}$H-magnetic resonance spectroscopy ($^{1}$H-MRS). Among these innovative techniques, MRI is a powerful non-invasive tool to monitor IntraMAT of the limbs or trunk in humans [11, 17]. Several MRI sequences, such as T1- and T2-weighted imaging, short-tau inversion recovery imaging, and two- or three-point Dixon imaging, have been used extensively to acquire anatomical information on the skeletal muscle and adipose tissue within the skeletal muscle in young and old healthy subjects as well as patients with neuromuscular disorders [6, 11, 17]. However, it is not known whether increased IntraMAT is due to an increase in adipocytes inside or outside of muscle cells, although increased lipids inside of muscle cells, that is, intramyocellular

lipids (IMCL), are known to have a negative impact on metabolism [18, 19]. Therefore, gaining this kind of information would be helpful for understanding the metabolism of IntraMAT, developing interventions to reduce the risk for type 2 diabetes, or even determining triggers for and a cure of myopathy [11, 17].

US is the less expensive test to estimate IntraMAT compared with other imaging techniques. If researchers or doctors cannot access an MRI, US is a substitutable methodology to estimate IntraMAT based on echo intensity [13, 20]. In earlier studies, Sipilä and Suominen [21, 22] showed that echo intensity of the quadriceps femoris is lower in elderly athletes than untrained individuals, suggesting elderly athletes have less IntraMAT content than healthy sedentary individuals. As with MRI, however, it is not clear that the origin of reflected echo of skeletal muscle sonography comes from in the muscle cells.

To resolve these questions, we used $^{1}$H-MRS to identify the location of adipocytes in muscle cells, that is, the IMCL and extramyocellular lipids (EMCL) [23, 24]. The usefulness and validity of physiological and biochemical significance of these fat components (IMCL and EMCL) using $^{1}$H-MRS has been extensively reviewed in the literature [23]. The purpose of this study was to assess relationships between IntraMAT content determined by MRI and IMCL and EMCL determined by $^{1}$H-MRS or echo intensity determined by US. We hypothesized that IntraMAT content determined by MRI and echo intensity by US would be related to IMCL, because IMCL has been shown to be a good index of lipid deposits within muscle cells in previous studies [23].

## 2. Materials and Methods

### 2.1 Subjects

Fifteen elderly (70.7 ± 3.8 years, 7 men and 8 women) and 15 young (20.9 ± 0.3 years 8 men and 7 women) men and women volunteered to participate in this study. The reason of we used elderly and young subjects was to get a wide range of values in variables to get better correlations. It should be noted that the range of variables in the two age groups was not polarized, which was as expected (Table 1). Before the experiment, the procedure, purposes, risks, and benefits associated with the study were explained and written consent was obtained. This study was approved by the Institutional Review Board of the local institute, and was conducted in accordance with the guidelines of the Declaration of Helsinki.

### 2.2 MRI acquisition and analysis

MRI was performed on a 3.0T (MAGNETOM Verio, Siemens Healthcare Diagnostics K.K., Tokyo, Japan) whole-body scanner. Subjects were placed in a supine position and images of the thigh were acquired using a body coil. T1-weighted spin-echo transaxial images of the right-thigh were collected with the following parameters: TR/TE 604/11 msec; voxel resolution 0.75 mm; optimized field of view 256 x 256 mm; slice thickness 10 mm; and interslice gap 0 mm. Representative images are shown in Figure 1.

Medical Image Processing, Analysis and Visualization software (version 4.4.0; National Institutes of Health, Bethesda, MD) was used to analyze images on a

personal computer (MacBook Pro, Apple Inc., Cupertino, CA). The MRI data analysis procedure was essentially the same as described previously [1, 11]. Briefly, we selected an image of the mid-thigh according to markers attached at the middle point between the greater trochanter and lateral condyle of the femur (see Figure 1) and identified vastus lateralis (VL) and biceps femoris-long head (BF). Contiguous axial images were used to help identify each of the muscles and the muscle boundaries.

We calculated the cross-sectional area (CSA) of skeletal muscle and IntraMAT content at the mid-thigh as described previously [1, 11]. The first step of the analysis was to correct for image heterogeneity caused by suboptimal radiofrequency coil uniformity, or gradient-driven eddy currents, using a well-established nonparametric nonuniform intensity normalization (N3) algorithm [1, 6, 11, 25]. This step was essential for subsequent analyses that assume homogenous signal intensity across images. Optimized image correction parameters (N3) were determined (end tolerance 0.0001; maximum iterations 100; signal threshold 1; field distance 25 mm; subsampling factor 4; Kernal full width half maximum of 0.15; Wiener filter noise 0.01), and the same parameters were applied to all images. The investigator then drew six region-of-interests (ROIs) of 25 $mm^2$ each, and three of six ROIs were placed on the VI and the other three ROIs were placed on the subcutaneous adipose tissue. The VI, which contains 99% of skeletal muscle tissue [11], was chosen so that we would obtain a pure skeletal muscle peak in the pixel number-signal intensity histogram. The total number of pixels within the six ROIs and a frequency distribution and histogram of all pixels and signal intensities were produced.

To separate muscle and adipose tissues in the pixel number-signal intensity histogram with minimal investigator bias, we implemented the Otsu threshold method, a reliable histogram shape-based thresholding technique used in medical imaging analysis [26]. To minimize manual tracing-induced errors on thresholding values, the mean of five trials was used, and the values were applied to VL and BF. After carefully tracing the edge of each muscle, the following parameters were calculated: 1) the total number of pixels within the ROI; 2) the number of pixels with a signal intensity lower than the threshold value (skeletal muscle), and 3) the number of pixels with a value higher than the threshold value (IntraMAT). The proportion of skeletal muscle and IntraMAT of VL and BF muscles was then calculated using the following equations:

IntraMAT content (%) = (IntraMAT pixel number) / [(skeletal muscle pixel number) + (IntraMAT pixel number)] x 100

All images were read in random order, and one investigator performed all analyses. Test-retest reliability of IntraMAT content has been reported elsewhere [1]. Briefly, intraclass correlation coefficients (ICC [2, 1]) in individual muscles at the mid-thigh for 10 subjects were 0.97 and 1.00 for VL and BF, respectively (all $p < 0.001$). The standard error of the measurement was 2.1% and 1.6% for VL and BF, respectively. The minimal difference between the first measurement and the second measurement were 5.8% and 4.6% for VL and BF, respectively.

### 2.3 $^{1}$H-Magnetic resonance spectroscopy

$^{1}$H-MRS experiments were performed on the same day of MRI experiments

using the same MR system. The $^{1}$H-MRS procedure has been reported elsewhere [24]. Briefly, IMCL of the right-thigh was measured by $^{1}$H-MRS using a 4-channel flex coil (366 × 174 mm). Voxels (11 × 11 × 20 mm) were positioned in the VL and BF at the mid-thigh between the greater trochanter and lateral condyle of the femur to match the position of MRI measurement. Care was taken to avoid visible vascular structures, adipose tissue deposits and connective tissues within the voxel. $^{1}$H-MRS spectra from regions of interest were acquired using a point-resolved spectroscopy sequence (PRESS) with the following acquisition parameters: TR/TE 4000/30 msec; 128 averages. The unsuppressed water signal was subsequently measured in the same voxel under the same shimming conditions. It was used as a reference signal [23].

Fitting of all $^{1}$H-MRS data was performed using LCModel (v.6.2-4A) [27]. The spectroscopic data acquired from the MR scanner were collected in a Linux computer, and metabolism was quantified using eddy current correction and water scaling. The concentration of water was assumed to be equal to 42.4 mmol/kg wet weight on the basis of a mean adult muscle tissue water content of 77% [28]. Concentrations of IMCL ($-CH_2$) and EMCL ($-CH_2$) were collected for the T1 and T2 relaxation effects of the unsuppressed water peak using LCModel control parameter atth2o, which were determined using the following equation: exp (-TE/T2) [1-ext (-TR/T1)] [29], assuming relaxation time T1 = 369 msec, T2 = 89.4 msec for the $IMCL_{CH2}$ and T1 = 369 msec, T2 = 77.6 msec for the $EMCL_{CH2}$ [30], respectively. The concentration of lipid molecules (total lipid content) was computed by the summation of the $IMCL_{CH2}$ and $EMCL_{CH2}$ concentrations and division by factor 31. The value 31

follows from the assumption that the average number of methylene protons is 62 per triglyceride molecule (equivalent to 31 $CH_2$ groups) [31-33]. The data were converted from mM to mmol/kg wet weight, assuming a tissue density 1.05 g/mL for skeletal muscle [32]. We acquired IMCL and EMCL data from the VL and BF of all 15 of the younger individuals and of 12 and 14 of the elderly individuals, respectively.

**2.4 Ultrasonography measurement and analysis**

A real-time B-mode ultrasonography (LOGIQ e, GE Healthcare, USA) with a 8-12 MHz linear-array probe (width of probe, 6 cm) was used to examine the echo intensity of VL and BF of the right mid-thigh matching the same location of MRI and $^1$H-MRS measurements. US images were scanned using the following acquisition parameters: frequency 8 MHz; gain 80 dB; depth 8 cm; number of focus point 1 (top of the image). Body hair at skin surfaces on measurement sites was shaved to minimize unwanted reflection echo. All measurements for the VL and BF were carried out with subjects in supine and prone positions, respectively. The probe was coated with an adequate water-soluble transmission gel to provide acoustic contact without depression of the dermal surface and was aligned perpendicular to the VL and BF to obtain transverse images. Five images were obtained for each muscle. Ultrasound images were stored in an ultrasound machine with the DICOM format for future analysis.

Image files were stored on a personal computer and echo intensity was analyzed using ImageJ (version 1.44; National Institutes of Health, Bethesda, MD). The first step of analysis involved smoothing to convert originally established grey-scale in

an ultrasound image to 256 grey-scale level on ImageJ. The region of interest (ROI), which included as much muscle as possible but avoided visible bone and fascia, was determined using polygon selections to calculate echo intensity [34]. Mean grey-scale levels within a ROI were used for echo intensity, which was expressed in arbitrary units as a value between 0 and 255. The mean value of echo intensity in five images for each muscle was used for analysis.

**2.5 Statistical analysis**

All values are reported as means and standard deviation. The student paired t test was used for differences in parameters between the VL and BF. Pearson product-moment correlation coefficients were used to determine the association between variables. The level of significance was set at $P < 0.05$. All statistical analyses were performed using IBM SPSS Statistics (version 21.0, IBM Japan, Tokyo, Japan).

## 3. Results

IntraMAT content, EMCL, and echo intensity in the BF were 3.5-, 2.3-, and 1.2-fold, respectively, higher than that of the VL ($P < 0.001$) (Table 1). There was no significant difference in IMCL between the VL and BF.

There was a significant correlation between IntraMAT content and EMCL ($r = 0.506$, $P < 0.01$) in the VL; however, there was no significant correlation between IntraMAT content and IMCL ($r = 0.263$, n.s.) (Figure 2). Similar to the VL, there was a significant correlation between IntraMAT content and EMCL ($r = 0.591$, $P < 0.001$) in the BF; however, there was no significant correlation between IntraMAT content and IMCL ($r = 0.236$, n.s.) (Figure 3).

Regarding echo intensity, the results were the same as those regarding the relation between IntraMAT content and IMCL or EMCL in the VL and BF. There was a significant correlation between echo intensity and EMCL (VL, $r = 0.485$, $P < 0.01$; BF, $r = 0.648$, $P < 0.001$) in the VL and BF; however, there was no significant correlation between echo intensity and IMCL (VL, $r = 0.060$ and BF, $r = 0.341$) (Figures 4 and 5).

IntraMAT content was correlated with echo intensity in the VL and BF (VL, $r = 0.404$, $P < 0.05$; BF, $r = 0.493$, $P < 0.01$) (Figure 6).

## 4. Discussion

The purpose of this study was to assess relationships among IntraMAT content, echo intensity, and IMCL and EMCL. IntraMAT content or echo intensity was significantly correlated with EMCL ($r = 0.458$ to $0.506$, $P < 0.01$ for the VL and $r = 0.591$ to $0.648$, $P < 0.001$ for the BF). Contrary to our hypothesis, there was no significant relation between IntraMAT content or echo intensity and IMCL ($r = 0.060$ to $0.341$) in any muscle. We also found that IntraMAT content was significantly correlated with echo intensity. This result clearly showed that information about intramuscular adipose tissue determined by MRI and US, which are valuable non-invasive methodologies in research and diagnosis, primarily represent information on lipids outside of muscle cells, as opposed to inside muscle cells.

### 4.1 IntraMAT and IMCL or EMCL relationship

MRI has been widely used to evaluate quality and quantity of skeletal muscle as a result of aging [1-4], inactivity [5, 6], obesity [7-10], myopathy [11-13], and orthopedic-related disuse [35]. MRI is a powerful tool to quantify size of muscle, fat or other tissues in T1-weighted images using image analysis techniques [1, 4, 6, 11]. To accomplish this segmentation analysis, several algorithms have been proposed in the literature [1, 4, 11, 36-38]. In this study, we used a reliable histogram shape-based thresholding technique that was used in previous studies [1, 11]. Using this technique, we clearly showed that IntraMAT content was significantly correlated with adipose tissue accumulated outside of muscle cells, that is, EMCL, but not inside of muscle cells,

that is, IMCL, for both the VL and BF. This result did not support our hypothesis; however, the finding provides crucial information in terms of metabolism of adipose tissue within skeletal muscle.

In this study, IMCL content of our subjects was 9.4 ± 4.9 mmol/kg wet weight for the VL (younger only: 8.5 ± 1.6 mmol/kg wet weight) and 10.5 ± 7.7 mmol/kg wet weight for the BF (younger only: 7.7 ± 1.1 mmol/kg wet weight). These values are comparable with Jacobs et al. [18], who reported that IMCL content of the soleus muscle in subjects with increased insulin-sensitive (mean age, 32 years) was 6.4 ± 0.6 mmol/kg wet weight. For young individuals, IMCL content in our subjects was similar to this previous study. In terms of EMCL, only a few studies have reported values. Our elderly subjects had a 2.7-fold higher EMCL in the VL compared with younger subjects (young: 21.9 ± 3.3 mmol/kg wet weight). Jacobs et al. [18] showed EMCL content of he soleus was 10.7 ± 1.6 mmol/kg wet weight, which was approximately half of young individuals in this study. However, this could be due to physical characteristics, physical activity level, and/or muscle specific functional roles during daily life. Overall, we recognized that our IMCL and EMCL content could be within normal ranges.

IntraMAT content is positively associated with insulin resistance and increased levels are a risk factor for type 2 diabetes [7, 8, 39]. Accordingly, EMCL may have a significant effect on insulin resistance of skeletal muscle. To support this hypothesis, Sinha et al. [40] reported a significant negative correlation between insulin sensitivity and EMCL ($r = -0.53$). Interestingly, studies have also shown a significant positive correlation between IMCL [18, 19] and insulin resistance even though EMCL

and IMCL have different associations with IntraMAT content in this study.

A correlation study that combined MRI with histochemical analysis showed a relation between IntraMAT by MRI and the content of adipose tissue in corresponding muscle biopsy samples. Rossi et al. [41] reported that IntraMAT content was closely related with adipocyte area by histology of muscle specimens ($r = 0.84$, $P < 0.001$). However, their study did not identify the exact location of adipocytes on histological sections under microscope observation.

**4.2 Echo intensity and IMCL or EMCL relationship**

A novel finding of this study was that the echo intensity determined by skeletal muscle US was significantly correlated with EMCL, but not IMCL, suggesting that the reflected echo mainly came from adipose tissue outside of muscle cells, not inside. This finding may also be strengthened by our finding that the amount of EMCL was 2.6- to 9.7-fold higher than IMCL in our subjects (Table 1). This result is important because, similar to MRI, echo intensity could be used as an index of IntraMAT content as done in previous studies [20, 42, 43]. In these previous studies, increased echo intensity was thought to be primarily caused by increases in adipose tissue and/or connective tissue within a muscle [20, 42, 43]; however, it is not well understood whether echo intensity is associated with adipose and/or connective tissues within a muscle. This study revealed that increased echo intensity of skeletal US is primarily due to extramyocellular adipose tissue.

In terms of connective tissue within a muscle, Reimers et al. [44] determined

that the morphologic basis of increased echo intensity is due to lipomatosis or fibrosis by histochemical analysis (relative area of fat cells within total cross-sectional area in transverse sections of muscle samples) of 86 biopsy samples from five lower and upper limb muscles such as the VL and biceps brachii. They showed that lipomatosis, that is, increased IntraMAT content, is a major predictor to account for increased echo intensity of muscle US, but that fibrosis did not significantly affect increased echo intensity. Furthermore, they showed that there was a significant relation between echo intensity and IntraMAT content determined by biochemical analysis ($r = 0.56$, $P < 0.01$). Taken together, echo intensity by US primarily represents adipose tissue outside of the muscle cells, which is similar results found on MRI.

### 4.3 IntraMAT and echo intensity relationship

It is important to note that there was a significant relationship between IntraMAT content determined by T1-weighted MRI and echo intensity for both the VL ($r = 0.404$, $P < 0.05$) and BF ($r = 0.493$, $P < 0.01$).

The value of quantifying IntraMAT content using MRI or US is that IntraMAT content is a negatively associated with muscle function in previous studies [6, 13, 14, 24, 42, 45-47]. Rech et al. [45] showed a significant negative correlation between echo intensity of the VL and maximum voluntary contraction of knee extension in 55 healthy women ($r = -0.399$, $P < 0.01$), implying individuals with higher IntraMAT content had lower muscle strength of the quadriceps femoris. Regarding IntraMAT content by MRI, Tuttle et al. [48] showed that a negative correlation between

increased levels of IntraMAT and decreased strength of the calf in healthy obese individuals, subjects with diabetes mellitus, and subjects with peripheral neuropathy ($r = -0.36$, $P < 0.05$). Similarly, the IntraMAT cross-sectional area in the thigh by MRI was related to mobility function including 6-minute walking distance ($r = -0.33$, $P < 0.01$), stair ascent time ($r = 0.39$, $P < 0.01$), stair decent time ($r = 0.36$, $P < 0.01$), and the timed up-and-go test ($r = 0.30$, $P < 0.01$) in 109 older adults [47].

In light of the evidence, skeletal muscle US may be substitutable for MRI for measurement of IntraMAT if researchers or doctors do not have access to MRI technology in a facility. In this case, it is important to note that care must be taken to avoid errors of measurement as suggested by Pillen et al. [13]. They proposed a generous amount of echo gel should be used to ensure optimal acoustic coupling and posture and anatomical location of measurement site should be identical for all subjects to prevent measurement errors. In addition, some other technical aspects such as pressure and angle of a probe could be influenced on echo intensity. Reflected echo attenuation by subcutaneous fat should also be accounted for when analyzing images.

In conclusion, results of this work demonstrate that IntraMAT content determined by T1-weighted MRI is related to EMCL and echo intensity of skeletal muscle on US. Furthermore, lipid deposits within muscle cells may not mainly affect IntraMAT content. These results suggest that IntraMAT content determined by T1-weighted MRI primarily reflects extramyocellular lipids.

Acknowledgements

The authors thank the volunteers for participation, Professor Kiyoshi Shimaoka and Ms. Nana Kanehira, Tokai Gakuen University, and Drs Haruo Isoda and Atsushi Fukuyama and Radiologic technologist Mr. Akira Ishizuka, Nagoya University. This study was supported in part by a Grant-in-Aid for challenging Exploratory Research from the Ministry of Education, Culture, Sports and Science and Technology Grant (#23650432) to HA.

The authors declare no conflict of interest.

References


1. Akima H, Yoshiko A, Hioki M, Kanehira N, Shimaoka K, Koike T et al. Skeletal muscle size is a major predictor of intramuscular fat content regardless of age. Eur J Appl Physiol 2015;
2. Crane JD, Devries MC, Safdar A, Hamadeh MJ, Tarnopolsky MA. The effect of aging on human skeletal muscle mitochondrial and intramyocellular lipid ultrastructure. J Gerontol A Bio Sci Med Sci 2010; 65A:119-28.
3. DeNino WF, Ades PA, Tchernof A, Sites CK, Dionne IJ, Poehlman ET et al. Contribution of abdominal adiposity to age-related differences in insulin sensitivity and plasma lipids in healthy nonobese women. Diabetes Care 2001; 24:925-32.
4. Kent-Braun JA, Ng AV, Young H. Skeletal muscle contractile and noncontractile components in young and older women and men. J Appl Physiol 2000; 88:662-8.
5. Akima H, Hioki M, Furukawa T. Effect of arthroscopic partial meniscectomy on the function of quadriceps femoris. Knee Surg Sports Traumatol Arthrosc 2008; 16:1017-25.
6. Manini TM, Clark BC, Goodpaster BH, Ploutz-Snyder LL, Harris TB. Reduced physical activity increases intermuscular adipose tissue in health young adults. Am J Nutr 2007; 85:377-84.
7. Goodpaster BH, Krishnaswami S, Resnick DE, Haggerty C, Harris TB, Schwartz AV et al. Association between regional adipose tissue distribution and both type 2 diabetes and impaired glucose tolerance in elderly men and women. Diabetes Care 2003; 26:372-9.
8. Goodpaster BH, Thaete FL, Kelley DE. Thigh adipose tissue distribution is associated with insulin resistance in obesity and in type 2 diabetes mellitus. Am J Clin Nutr 2000; 71:885-92.
9. Goodpaster BH, Wolf D. Skeletal muscle lipid accumulation in obesity, insulin resistance, and type 2 diabetes. Pediatr Diabetes 2004; 5:219-26.
10. Janssen I, Fortier A, Hudson R, Ross RR. Effects of an energy-restrictive diet with or without exercise on abdominal fat, intermuscular fat, and metabolic risk factors in obese women. Diabetes Care 2002; 25:431-8.

11. Akima H, Lott D, Senesac C, Deol J, Gemain S, Arpan I et al. Relationships of thigh muscle contractile and non-contractile tissue with function, strength, and age in boys with Duchenne muscular dystrophy. Neuromuscul Disord 2012; 22:16-25.
12. McDonald CM, Abresch RT, Carter GT, Fowler WM, Johnson ER, Kilmer DD et al. Profiles of neuromuscular diseases. Duchenne muscular dystrophy. Am J Phys Med Rehabil 1995; 74 (5 Suppl):S70-S92.
13. Pillen S, Arts IMP, Zwarts MJ. Muscle ultrasound in neuromuscular disorder. Muscle Nerve 2008; 37:679-93.
14. Addison O, Marcus RL, LaStayo P, Ryan AS. Intermuscular fat: a review of the consequences and causes. Inter J Endocrinol 2014; 2014:309570.
15. Ryan AS, Nicklas BJ. Age-related changes in fat deposition in mid-thigh muscle in women: relationships with metabolic cardiovascular disease risk factors. Int J Obes 1999; 23:126-32.
16. Miljkovic I, Cauley JA, Petit MA, Ensrud KE, Strotmeyer E, Sheu Y et al. Greater adipose tissue infiltration in skeletal muscle among older men of African ancestry. J Clin Endocrinol Metab 2009; 94:2735-42.
17. Mercuri E, Pichiecchio A, Allsop J, Messina S, Pane M, Muntoni F. Muscle MRI in inherited neuromuscular disorders: past, present, and future. J Magn Reson Imaging 2007; 25:433-40.
18. Jacob S, Machann J, Rett K, Brechtel K, Volk A, Renn W et al. Association of increased intramyocellular lipid content with insulin resistance in lean nondiabetic off spring of type 2 diabetic subjects. Diabetes 1999; 48:1113-9.
19. Lawrence JC, Newcomer BR, Buchthal SD, Sirikul B, Oster RA, Hunter GR et al. Relationship of intramyocellular lipid to insulin sensitivity may differ with ethnicity in healthy girls and women. Obesity (Silver Spring) 2011; 19:43-8.
20. Arts IMP, Pillen S, Schelhaas HJ, Overeem S, Zwarts MJ. Normal values for quantitative muscle ultrasonography in adults. Muscle Nerve 2010; 41:32-41.
21. Sipilä S, Suominen H. Ultrasound imaging of the quadriceps muscle in elderly athletes and untrained men. Muscle Nerve 1991; 14:527-33.
22. Sipilä S, Suominen H. Muscle ultrasonography and computed tomography in elderly trained and untrained women. Muscle Nerve 1993; 16:294-300.

23. Boesch C, Machann J, Vermathen P, Schick F. Role of proton MR for the study of muscle lipid metabolism. NMR Biomed 2006; 19:968-88.
24. Hioki M, Kanehira N, Koike T, Saito A, Takahashi H, Shimaoka K et al. Associations of intramyocellular lipid in vastus lateralis and biceps femoris with blood free fatty acid and muscle strength differ between young and elderly adults. Clin Physiol Func Imaging 2015;
25. Sled JG, Zijdenbos AP. A nonparametric method for automatic correction of intensity nonuniformity in MRI data. IEEE Trans Med Imaging 1998; 17:87-97.
26. Sezgin M, Sankur B. Survey over image thresholding techniques and quantitative performance evaluation. J Electro Imaging 2004; 13:146-65.
27. Provencher SW. Estimation of metabolite concentrations from localized in vivo proton NMR spectra. Magn Reson Med 1993; 30:672-9.
28. Sjøgaard G, Saltin B. Extra- and intracellular water spaces in muscles of man at rest and with dynamic exercise. Am J Physiol Regul Integr Comp Physiol 1982; 243:R217-R80.
29. Drost DJ, Riddle WR, Clarke GD. Proton magnetic resonance spectroscopy in the brain: report of AAPM MR Task Group #9. Med Phys 2002; 29:2177-97.
30. Krssak M, Mlynarik V, Meyerspeer M, Moser E, Roden M. 1H NMR relaxation times of skeletal muscle metabolites at 3 T. Magma 2004; 16:155-9.
31. Boesch C, Decombaz J, Slotboom J, Kreis R. Observation of intramyocellular lipids by means of 1H magnetic resonance spectroscopy. Proc Nutr Soc 1999; 58:841-50.
32. Szczepaniak LS, Babcock EE, Schick F, Dobbins RL, Garg A, Burns DK et al. Measurement of intracellular triglyceride stores by H spectroscopy: validation in vivo. Am J Physiol 1999; 276:E977-89.
33. Weis J, Johansson L, Ortiz-Nieto F, Ahlstrom H. Assessment of lipids in skeletal muscle by LCModel and AMARES. J Magn Reson Imaging 2009; 30:1124-9.
34. Caresio C, Molinari F, Emanuel G, Minetto MA. Muscle echo intensity: reliability and conditioning factors. Clin Physiol Func Imaging 2014;
35. Akima H, Furukawa T. Atrophy of thigh muscles after meniscal lesions and arthroscopic partial meniscectomy. Knee Surg Sports Traumatol Arthrosc 2005; 13:632-7.

36. Gorgey AS, Dudley GA. Skeletal muscle atrophy and increased intramuscular fat after incomplete spinal cord injury. Spinal Cord 2007; 45:304-9.
37. Holmback AM, Askaner K, Holtas S, Downham D, Lexell J. Assessment of contractile and noncontractile components in human skeletal muscle by magnetic resonance imaging. Muscle Nerve 2002; 25:251-8.
38. Manini TM, Buford TW, Lott DJ, Vandenborne K, Daniels MJ, Knaggs JD et al. Effect of dietary restriction and exercise on lower extremity tissue compartments in obese, older women: A pilot study. J Gerontol A Bio Sci Med Sci 2013; 69:101-8.
39. Ryan AS, Buscemi A, Forrester L, Hafer-Macko CE, Ivey FM. Atrophy and intramuscular fat in specific muscles of the thigh: associated weakness and hyperinsulinemia in stroke survivors. Neurorehabil Neural Repair 2011; 25:865-72.
40. Sinha R, Dufour S, Petersen KF, LeBon V, Enoksson S, Ma Y-Z et al. Assessment of skeletal muscle triglyceride content by 1H nuclear magnetic resonance spectroscopy in lean and obese adolescents. Relationships to insulin sensitivity, total body fat, and central adiposity. Diabetes 2002; 51:1022-7.
41. Rossi A, Zoico E, Goodpaster B, Sepe A, Di Francesco V, Fantin F et al. Quantification of intermuscular adipose tissue in the erector spinae muscle by MRI: agreement with histology evaluation. Obesity 2010; 18:2379-84.
42. Fukumoto Y, Ikezoe T, Yamada Y, Tsukagoshi R, Nakamura M, Mori N et al. Skeletal muscle quality assessed from echo intensity is associated with muscle strength of middle-aged and elderly persons. Eur J Appl Physiol 2012; 112:1519-25.
43. Pillen S, van Dijk JP, Weijerts G, Raijmann W, de Korte CL, Zwarts MJ. Quantitative gray-scale analysis in skeletal muscle ultrasound: a comparison study of two ultrasound devices. Muscle Nerve 2009; 39:781-6.
44. Reimers K, Reimers CD, Wagner S, Paetzke I, Pongratz DE. Skeletal muscle sonography: a correlative study of echogenicity and morphology. J Ultrasound Med 1993; 2:73-7.
45. Rech A, Radaelli R, Goltz FR, da Rosa LH, Schneider CD, Pinto RS. Echo intensity is negatively associated with functional capacity in older women. Age (Dordr) 2014; 36:9708.

46. Wilhelm EN, Rech A, Minozzo F, Radaelli R, Botton CE, Pinto RS. Relationship between quadriceps femoris echo intensity, muscle power, and functional capacity of older men. Age (Dordr) 2014; 36:9625.
47. Marcus RL, Addison O, Dibble LE, Foreman KB, Morrell G, LaStayo P. Intramuscular adipose tissue, sarcopenia, and mobility function in older individuals. J Aging Res 2012; 2012:1-6.
48. Tuttle LJ, Sinacore DR, Mueller MJ. Intermuscular adipose tissue is muscle specific and associated wtih poor functional performance. J Aging Res 2012; 2012:1-7.

1

2

3

Table 1 Intramuscular adipose tissue (IntraMAT) content, intramyocellular lipid (IMCL), extramyocellular lipid (EMCL), and echo intensity

| | Mean ± SD | | | Range | |
|---|---|---|---|---|---|
| | | | | Young | Old |
| Vastus lateralis | | | | | |
| IntraMAT (%) | 4.6 | ± | 3.0 | 0.7 - 5.3 | 1.8 - 13.7 |
| IMCL (mmol/kg wet weight)[1] | 9.4 | ± | 4.9 | 2.4 - 26.3 | 6.7 - 14.9 |
| EMCL (mmol/kg wet weight) | 40.2 | ± | 30.5 | 3.3 - 47.5 | 24.7 - 122.0 |
| Echo intensity (a.u.) | 61.1 | ± | 13.3 | 29.2 - 70.3 | 50.3 - 88.2 |
| | | | | | |
| | | | | | |
| Biceps femoris | | | | | |
| IntraMAT (%) | 16.2 | ± | 7.1† | 5.1 - 23.0 | 10.7 - 29.7 |
| IMCL (mmol/kg wet weight) | 10.5 | ± | 7.7 | 1.5 - 16.7 | 1.9 - 31.9 |
| EMCL (mmol/kg wet weight)[2] | 94.0 | ± | 56.2† | 13.9 - 143.9 | 29.5 - 202.3 |
| Echo intensity (a.u.) | 74.2 | ± | 14.1† | 35.2 - 81.7 | 77.0 - 100.1 |

†, $P < 0.001$ vs. vastus lateralis. 1, n =12, 2, n =14.

Figure legends

Figure 1 Representative T1-weighted MR images (spin-echo; repetition time, 604 msec; echo time 11 msec; field of view 256 x 256 mm; slice thickness 10 mm) of young (a) men and elderly men (b)

Note that the four markers on the lateral side of the thigh were used to identify the middle length of the thigh. VL, vastus lateralis; BF, biceps femoris. Scale 5 cm.

Figure 2 Relationship between intramuscular adipose tissue content determined by histogram shape-based thresholding technique of T1-weighted MRI and extramyocellular lipids (EMCL) or intramyocellular lipids (IMCL) determined by $^{1}$H-magnetic resonance spectroscopy in the vastus lateralis

Figure 3 Relationship between intramuscular adipose tissue content determined by histogram shape-based thresholding technique of T1-weighted MRI and extramyocellular lipids (EMCL) or intramyocellular lipids (IMCL) determined by $^{1}$H-magnetic resonance spectroscopy in the biceps femoris

Figure 4 Relationship between echo intensity determined by B-mode ultrasonography and extramyocellular lipids (EMCL) or intramyocellular lipids (IMCL)

determined by $^{1}$H-magnetic resonance spectroscopy in the vastus lateralis

Figure 5 Relationship between echo intensity determined by B-mode ultrasonography and extramyocellular lipids (EMCL) or intramyocellular lipids (IMCL) determined by $^{1}$H-magnetic resonance spectroscopy in the biceps femoris

Figure 6 Relationship between intramuscular adipose tissue content determined by histogram shape-based thresholding technique of T1-weighted MRI and echo intensity determined by B-mode ultrasonography in the vastus lateralis (VL) and biceps femoris (BF)

1 Figure 1

2

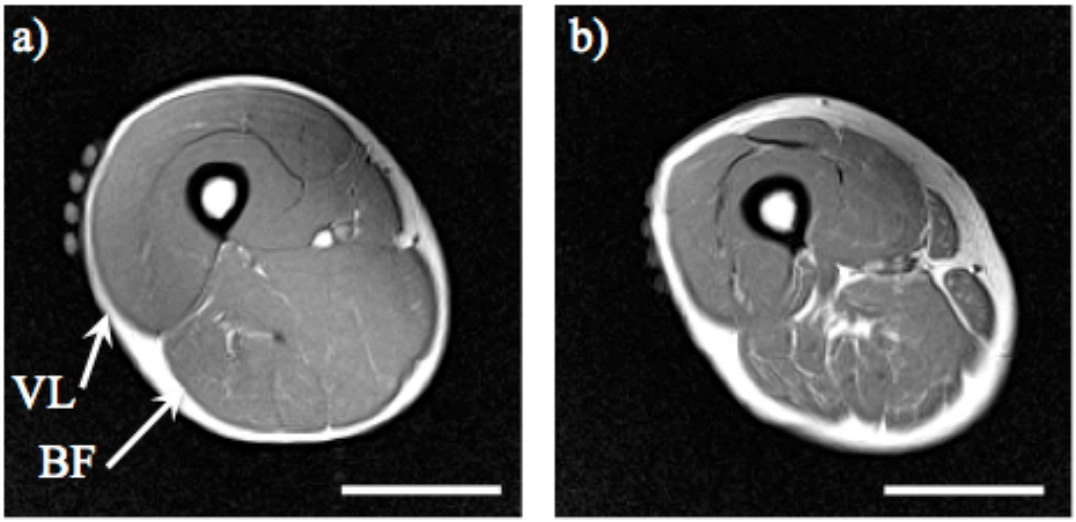


Figure 1

3

4

1 Figure 2

2

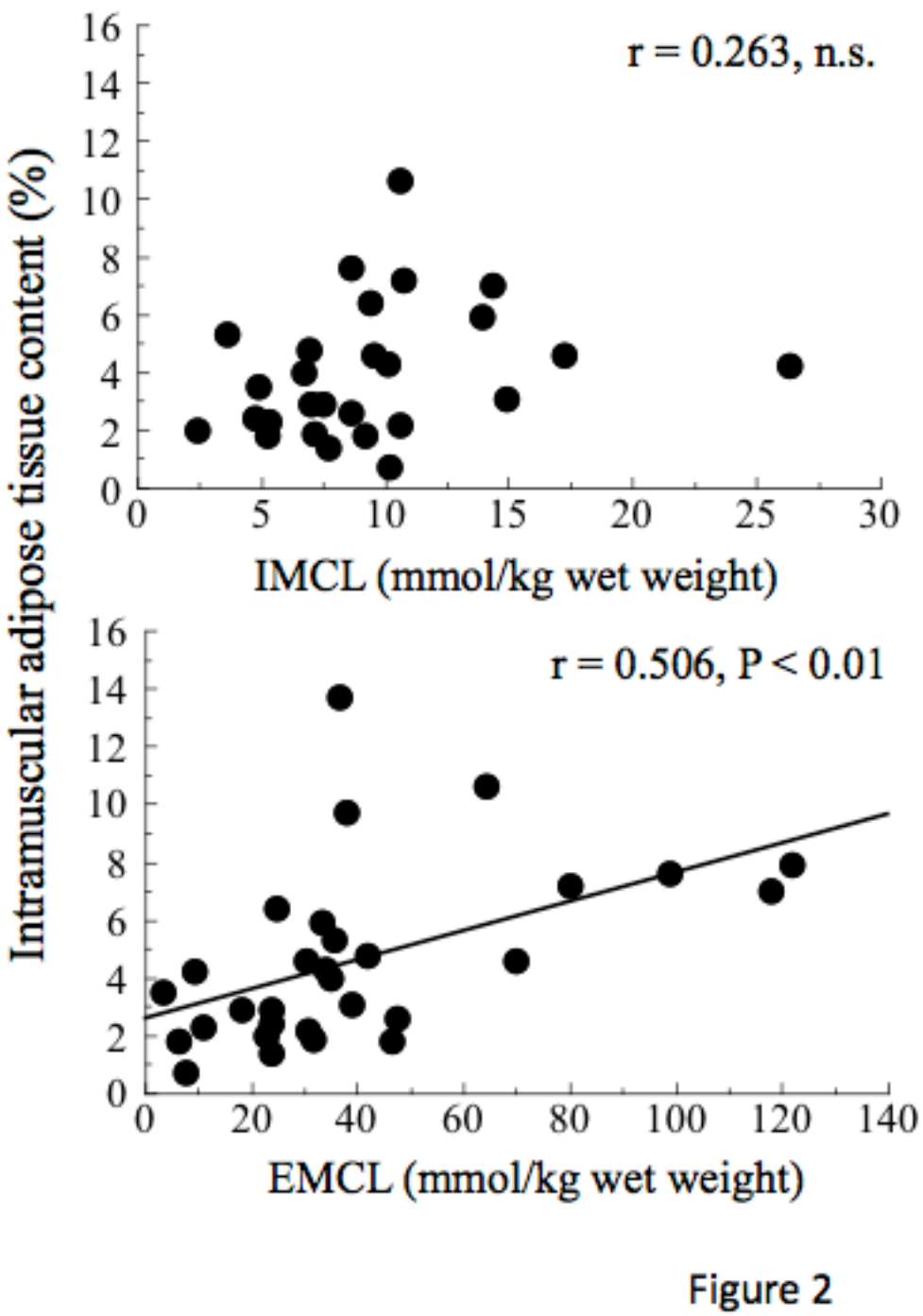


Figure 2

3

4

1 Figure 3

2

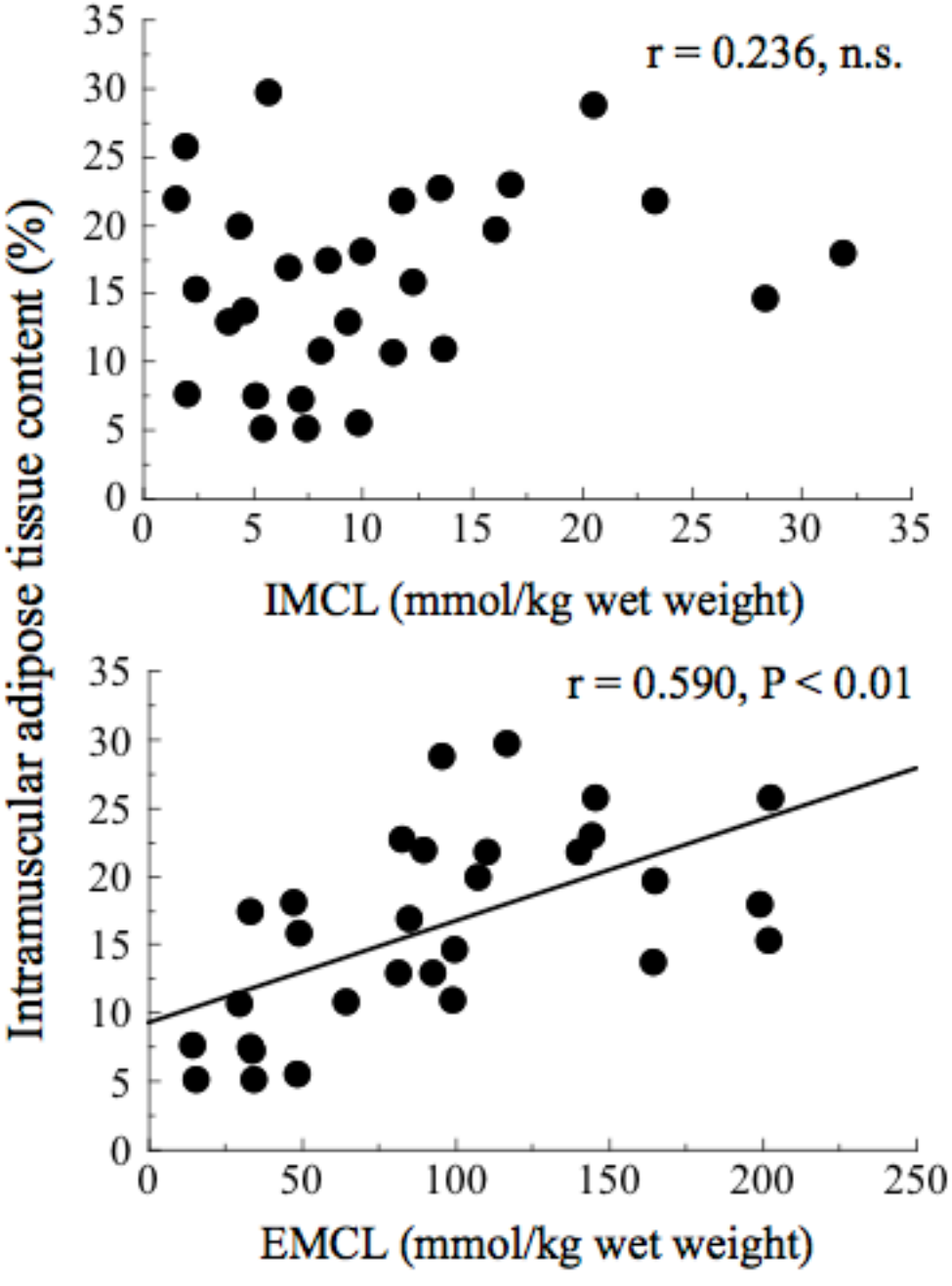


Figure 3

3

1 Figure 4

2

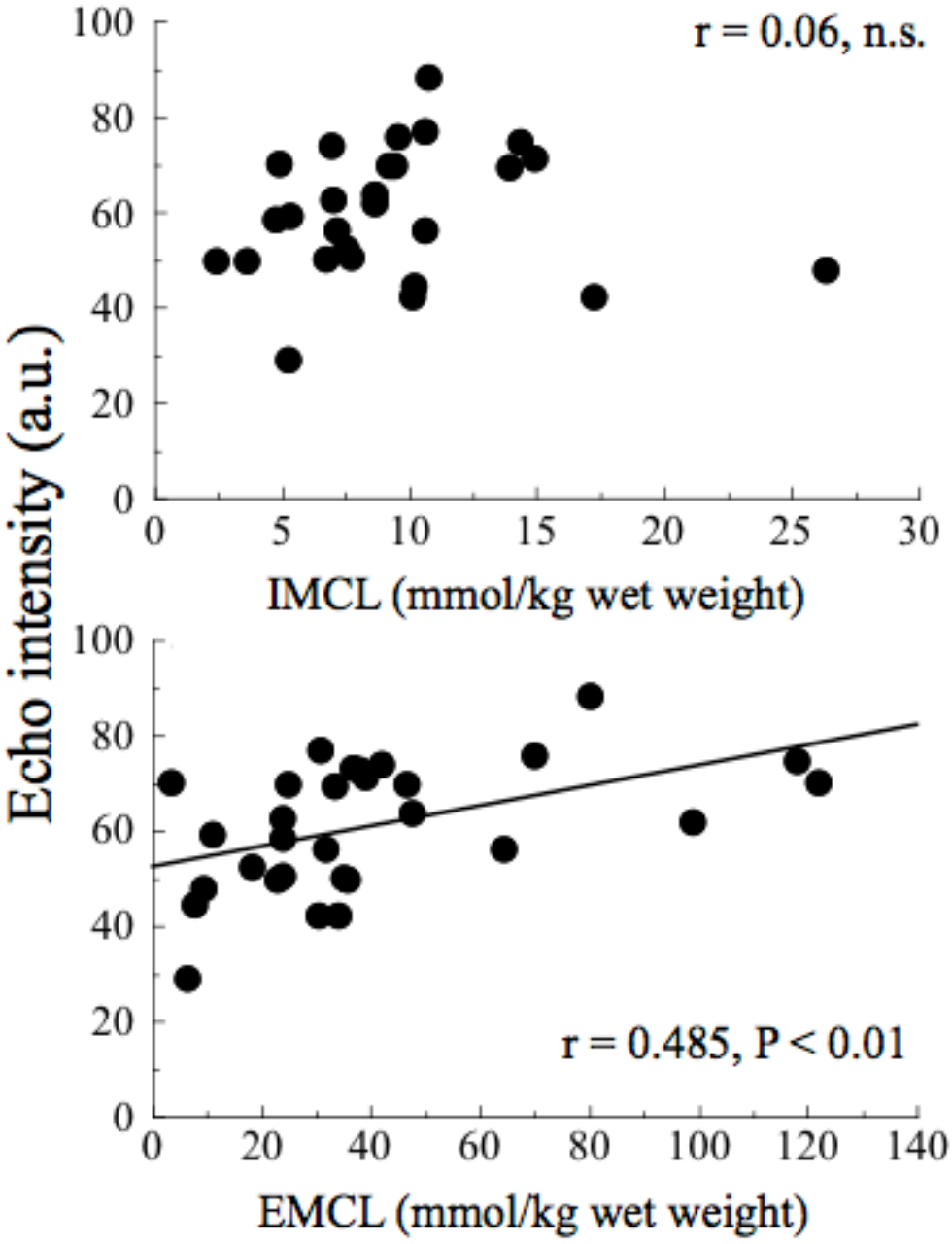


Figure 4

1 Figure 5

2

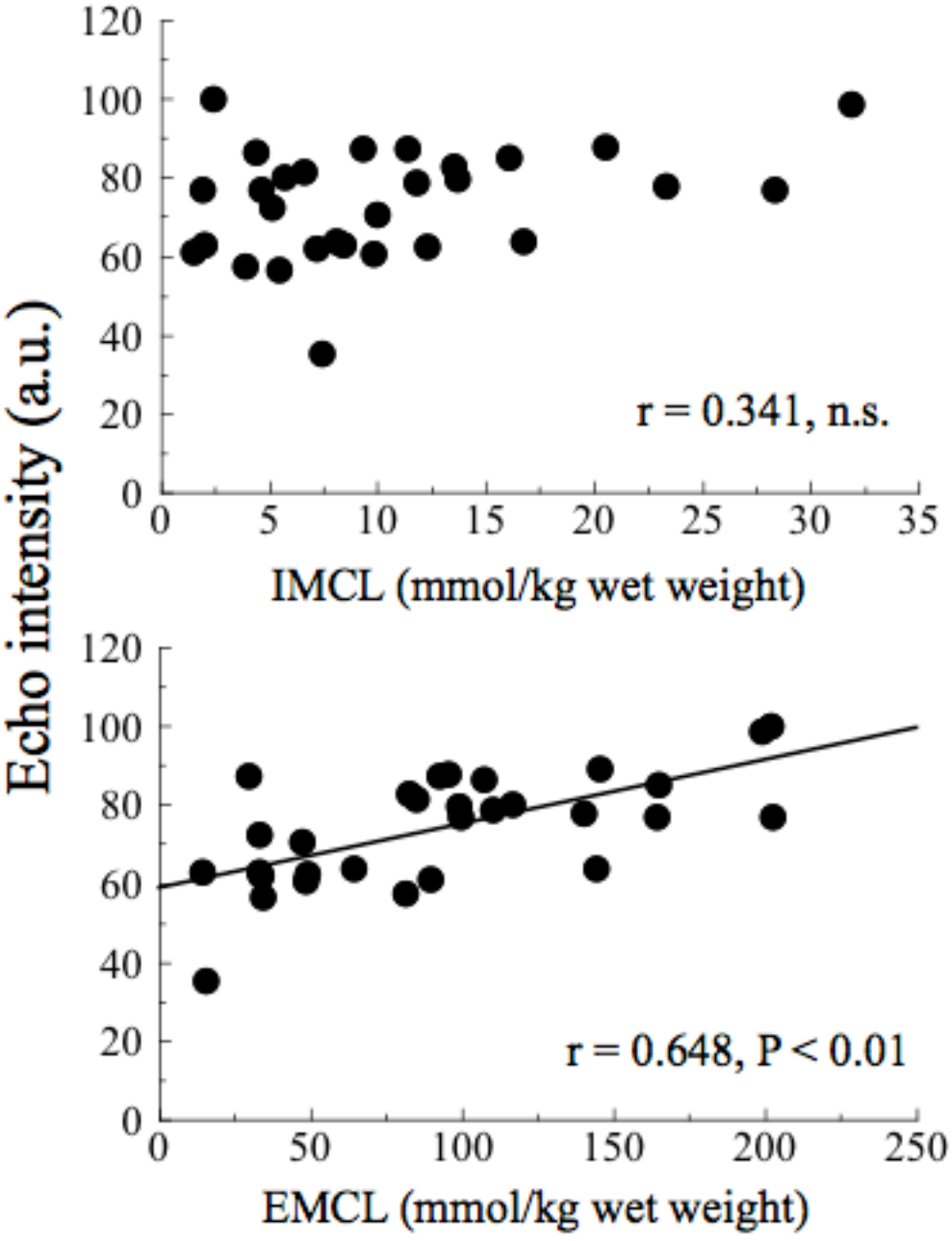


Figure 5

1 Figure 6

2

3

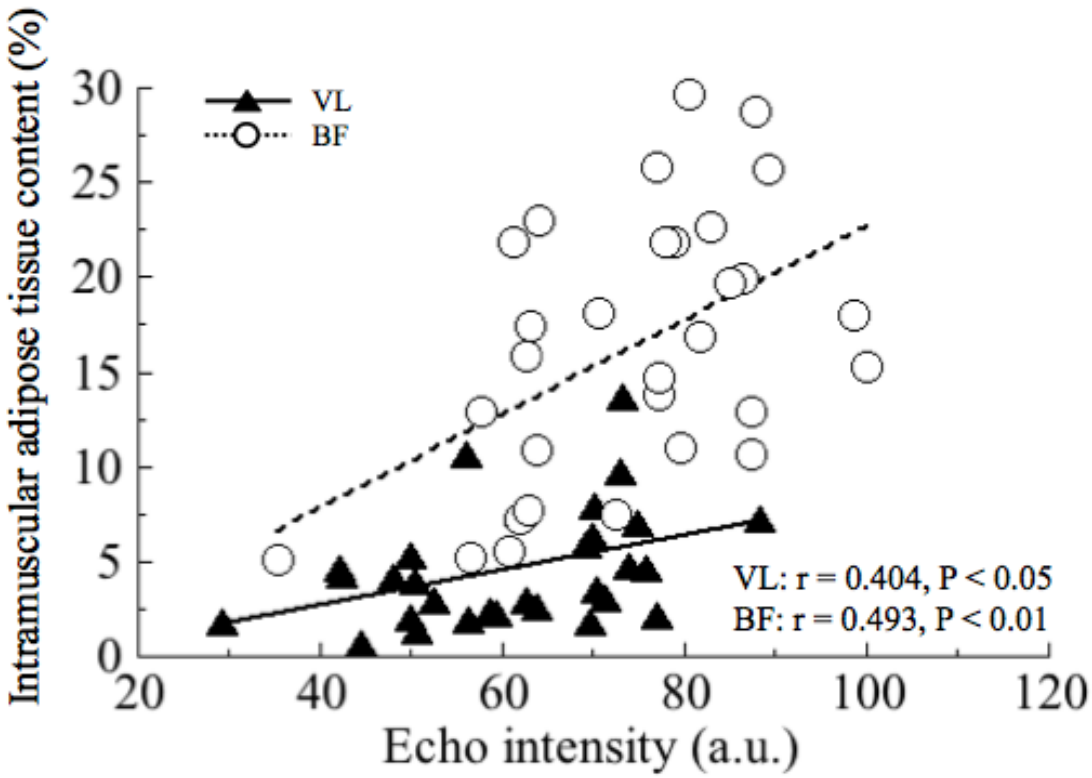


Figure 6